

# Coherent interfacial energy and composition profiles in ternary FCC systems by a discrete lattice plane analysis

Z.-G. YANG\*, T.-J. WANG, S. ZHONG

*Department of Materials Science and Engineering, Tsinghua University,  
Beijing 100084, P. R. China  
E-mail: zgyang@tsinghua.edu.cn*

G. YANG, G.-C. WANG

*Department of Materials Science and Engineering, Nanchang Aero Institute, Nanchang  
330034, P. R. China*

A discrete lattice plane, nearest neighbor, broken bond model which had been previously used to calculate the energy of coherent interphase boundaries in binary substitutional and ternary substitutional-interstitial systems was extended to ternary substitutional alloys to study the chemical interfacial energy and composition profiles across the interphase boundary in fcc solid solution. Compared with a binary system, the segregation of the third component atoms at the interphase boundary is demonstrated both with symmetric and asymmetrical composition profiles. Accordingly the interfacial energy is reduced by the presence of the third component. Increasing temperature has an effect of decreasing the gradient of composition profiles across the interface, as well as absolute value and anisotropy of the interfacial energy in ternary system.

© 2005 Springer Science + Business Media, Inc.

## 1. Introduction

The composition and free energy of interphase boundaries are two of the most important properties in studying the interface behavior in solid phases, in addition to crystallographic relationship. However, only a few of experimental data on the composition profile and energy of solid-solid interphase boundaries are available by scanning Auger electron spectroscopy [1] and solid state wetting measurements [2]. Due to relatively experimental difficulty, more attentions have been paid on theoretical studies [3, 4]. One of the earliest theoretical attempts is the Becker equation [5], in which the energy of coherent interphase boundaries is calculated from the change in total bond energies across the interface upon joining two crystals. Following this scheme, a discrete lattice plane (DLP) approach was developed to analyze the composition and energy variation associated with interphase boundaries [6–8] and temperatures [9], which agrees with the continuum model by Cahn and Hilliard [10] at sufficient high temperatures.

On the base of the above methods developed in binary solid solutions, the DLP/NNBB model is extended to fcc-based and bcc-based ternary substitutional-interstitial systems for the application to carbides and nitrides of B1(NaCl) structure, e.g. TiC and VN etc., with austenite and ferrite [11–13]. The rather different

anisotropy of interfacial energy and composition from a binary system is demonstrated in these ternary alloys, which suggests the significant effect of the non-metallic atoms as third component.

In a ternary substitutional system, the segregation in the surface and grain boundaries of one component has been extensively studied [14] based mainly on Gibbs adsorption theory [15], from which detailed understanding about the composition profile and interfacial energy is limited. A discrete version of Cahn and Hilliard's continuum theory has been applied to Cu-Ag-Au [16] and Cu-Pb-X [1] alloys to study interfacial segregation and energy. Embedded atom method [17] was also employed to above system to calculate the solution energy of Au within the interface and to obtain relaxed atomic configurations, however, for more ternary substitutional systems in general, the interfacial energy and concentration distributions are still lacking with respect to the variation of temperature and orientations.

In this report equations for solute profiles in the boundary region are developed in substitutional ternary systems following the DLP/NNBB method previously reported [9, 11]. Then, they are solved in numerous cases considering the various interaction coefficients between the component elements. The results are discussed with an emphasis on the characteristics of the

\*Author to whom all correspondence should be addressed.

influence of interaction parameters on the solute profiles and the chemical energy of interphase boundaries.

## 2. Calculation method

Consider that a block of an fcc solid solution (termed as  $\alpha$  phase) is joined to another block of fcc compound ( $\beta$  phase). They are both initially homogeneous regular solid solutions and have the compositions which correspond to the ends of the equilibrium tie-line in the ( $\alpha + \beta$ ) two phase region of the A-B-C ternary phase diagram, where A, B and C denote substitutional metal atoms. It is assumed that the lattice of the  $\alpha$  phase and that of the  $\beta$  phase have an identical lattice parameter, are cube-cube oriented and thus, the interfaces between them are fully coherent.

After joining, the system achieves a metastable equilibrium solute distribution at a constant temperature, pressure and chemical potential of component atoms under the boundary condition that the compositions far from the boundary are equal to those of bulk equilibrium. The total free energy change  $\Delta F$  can be defined as,

$$\Delta F = \Delta H - T \Delta S \quad (1)$$

where  $\Delta H$  and  $\Delta S$  are the enthalpy and entropy changes of the system accompanying the net atomic movements required to reach the equilibrium configuration after forming the interface from the initial homogeneous state.  $T$  is the temperature. In the calculation procedure, first step is to determine the equilibrium phase boundary composition before joining as a reference state.

### 2.1. Calculation of equilibrium concentration at $\alpha/\beta$ phase boundary in ternary system

The free energy of a homogeneous ternary phase per lattice site is given by,

$$G = \frac{Z}{2} [(x^A)^2 e_{11} + (x^B)^2 e_{22} + (x^C)^2 e_{33}] + Z(x^A x^B e_{12} + x^A x^C e_{13} + x^B x^C e_{23}) + k_B T (x^A \ln x^A + x^B \ln x^B + x^C \ln x^C) \quad (2)$$

where  $Z$  is the total coordination number ( $Z = 12$  for an fcc lattice),  $x^A$ ,  $x^B$  and  $x^C$  are the concentration of A, B and C atoms, respectively ( $x^A + x^B + x^C = 1$ ),  $k_B$  is the Boltzmann constant,  $e_{ij}$  is the bond energy of an  $i - j$  pair ( $i, j = 1, 2$  and  $3$  for A, B and C atoms), which is assumed constant and identical no matter it is within  $\alpha$  phase,  $\beta$  phase or at the  $\alpha/\beta$  interface.

From this expression the chemical potential of component species in phase  $\nu$  ( $\nu = \alpha$  or  $\nu = \beta$ ) is obtained as,

$$\mu_\nu^A = \frac{Z}{2} e_{11} + Z \Delta e_{12} (x_\nu^B)^2 + Z \Delta_{23} x_\nu^B x_\nu^C + Z \Delta e_{13} (x_\nu^C)^2 + k_B T \ln x_\nu^A \quad (3a)$$

$$\mu_\nu^B = \frac{Z}{2} e_{22} + Z \Delta e_{12} (x_\nu^A)^2 + Z \Delta_{13} x_\nu^A x_\nu^C + Z \Delta e_{23} (x_\nu^C)^2 + k_B T \ln x_\nu^B \quad (3b)$$

and

$$\mu_\nu^C = \frac{Z}{2} e_{33} + Z \Delta e_{13} (x_\nu^A)^2 + Z \Delta_{12} x_\nu^A x_\nu^B + Z \Delta e_{23} (x_\nu^B)^2 + k_B T \ln x_\nu^C \quad (3c)$$

where  $\Delta e_{ij}$  and  $\Delta_{23}$  etc. are defined by,

$$\Delta e_{ij} = e_{ij} - \frac{e_{ii} + e_{jj}}{2} \quad \text{and} \quad (4)$$

$$\Delta_{23} = \Delta e_{12} + \Delta e_{13} - \Delta e_{23}$$

The  $\Delta e_{12}$  is related to the regular solution interaction coefficient,  $L$ , in an A-B binary alloy as  $L = Z N_a \Delta e_{12}$  and the critical temperature of a miscibility gap as  $T_c = L/2R = Z \Delta e_{12}/2k_B$  where  $N_a$  is the Avogadro's number and  $R$ , the gas constant.  $\Delta e_{12}$  is always assumed positive through this calculation, and two parameters  $r = \Delta e_{13}/\Delta e_{12}$  and  $p = \Delta e_{23}/\Delta e_{12}$  are introduced for convenience during the calculation.

The phase boundary concentration is achieved when the chemical potentials for each kind of atom are identical in both  $\alpha$  and  $\beta$  phases, which is readily calculated from Equation 3 at any temperatures.

### 2.2. Calculation of concentration profile in interphase boundary region

By forming the interface, the total enthalpy change is given by DLP/NNBB model as,

$$\Delta H = n_s \sum_i \Delta e_{12} \left[ -(x_i^B - x_\nu^B)^2 Z + \sum_j (x_i^B - x_{i+j}^B)^2 Z_j \right] + n_s \sum_i \Delta e_{13} \times \left[ -(x_i^C - x_\nu^C)^2 Z + \sum_j (x_i^C - x_{i+j}^C)^2 Z_j \right] + n_s \sum_i \Delta_{23} \left[ -(x_i^B - x_\nu^B)(x_i^C - x_\nu^C) Z + \sum_j \{(x_i^C - x_{i+j}^C)(x_i^B - x_{i+j}^B)\} Z_j \right] \quad (5)$$

where  $n_s$  is the number of atom sites per unit area of interface,  $x_i$  is the atomic fraction in the  $i$ 'th interfacial layer of B or C element (as indicated in the superscript),  $x_\nu$  is initial equilibrium concentration in bulk  $\alpha$  or  $\beta$  phases ( $\nu = \alpha$  for original  $\alpha$  phase planes and  $\nu = \beta$  for original  $\beta$  phase planes).  $Z_j$  is the coordination number in the  $j$ 'th layer to an atom in the  $i$ 'th plane.  $\sum_i$  denotes summation over the entire interface zone, which is described as those atomic layers whose solute concentration differs from that of either bulk  $\alpha$  or  $\beta$ .

The configurational entropy change of  $\nu$  phase is,

$$\Delta S = -n_s k_B \sum_i \left\{ (1 - x_i^B - x_i^C) \ln \frac{1 - x_i^B - x_i^C}{1 - x_v^B - x_v^C} + x_i^B \ln \frac{x_i^B}{x_v^B} + x_i^C \ln \frac{x_i^C}{x_v^C} \right\} \quad (6)$$

The equilibrium distribution of each elements is achieved when the first derivatives of the free energy change with respect to the concentration vanish, that is,

$$\frac{\partial F}{\partial x_i^B} = 0, \quad \text{and} \quad \frac{\partial F}{\partial x_i^C} = 0 \quad (7)$$

The substitution of Equations 5 and 6 in the above equations yields a set of non-linear equations to be solved simultaneously for  $x_i^B$  and  $x_i^C$ ,

$$\begin{aligned} & 2\Delta e_{12} \left\{ x_v^B Z - x_i^B Z_0 - \sum_j (x_{i+j}^B + x_{i-j}^B) Z_j \right\} \\ & + \Delta_{23} \left\{ x_v^C Z - x_i^C Z_0 - \sum_j (x_{i+j}^C + x_{i-j}^C) Z_j \right\} \\ & - k_B T \left\{ \ln \left( \frac{1 - x_i^C}{x_i^B} - 1 \right) - \ln \left( \frac{1 - x_v^C}{x_v^B} - 1 \right) \right\} = 0 \end{aligned} \quad (8a)$$

and,

$$\begin{aligned} & 2\Delta e_{13} \left\{ x_v^C Z - x_i^C Z_0 - \sum_j (x_{i+j}^C + x_{i-j}^C) Z_j \right\} \\ & + \Delta_{23} \left\{ x_v^B Z - x_i^B Z_0 - \sum_j (x_{i+j}^B + x_{i-j}^B) Z_j \right\} \\ & - k_B T \left\{ \ln \left( \frac{1 - x_i^B}{x_i^C} - 1 \right) - \ln \left( \frac{1 - x_v^B}{x_v^C} - 1 \right) \right\} = 0 \end{aligned} \quad (8b)$$

The determination of  $n_s$  and  $Z_j$  in an fcc lattice, which has been described in previous paper [9] already, will not be duplicated here.

### 2.3. Calculation of interfacial energy

After obtaining the equilibrium solute distribution, it is possible to calculate the interfacial energy from the free energy changes,

$$\sigma = \Delta H - T \Delta S \quad (9)$$

By incorporation of the enthalpy and entropy terms, the equation for interfacial energy is written as,

$$\begin{aligned} \sigma = n_s \sum_i \Delta e_{12} \left[ - (x_i^B - x_v^B)^2 Z + \sum_j (x_{i+j}^B - x_{i-j}^B)^2 Z_j \right] \\ + n_s \sum_i \Delta e_{13} \left[ - (x_i^C - x_v^C)^2 Z + \sum_j (x_{i+j}^C - x_{i-j}^C)^2 Z_j \right] \end{aligned}$$

$$\begin{aligned} & + n_s \sum_i \Delta_{23} \left[ - (x_i^B - x_v^B) (x_i^C - x_v^C) Z \right. \\ & \left. + \sum_j \{ (x_i^C - x_{i+j}^C) (x_i^B - x_{i+j}^B) \} Z_j \right] \\ & + n_s k_B T \sum_i \left\{ (1 - x_i^B - x_i^C) \ln \frac{(1 - x_i^B - x_i^C)}{(1 - x_v^B - x_v^C)} \right. \\ & \left. + x_i^B \ln \frac{x_i^B}{x_v^B} + x_i^C \ln \frac{x_i^C}{x_v^C} \right\} \end{aligned} \quad (10)$$

At  $T = 0$  K, the  $k_B T$  term vanishes and the solute profiles change abruptly across the interphase boundary. Then, Equation 10 is simplified to a Becker-type equation,

$$\begin{aligned} \sigma = n_s \Delta e_{12} (x_\alpha^B - x_\beta^B)^2 \sum_j j Z_j + n_s \Delta e_{13} (x_\alpha^C - x_\beta^C)^2 \\ \times \sum_j j Z_j + n_s \Delta_{23} (x_\alpha^B - x_\beta^B) (x_\alpha^C - x_\beta^C) \sum_j j Z_j \end{aligned} \quad (11a)$$

which at sufficiently low temperatures permits a quick estimate of  $\sigma$  to be made for various interface orientations once the bulk equilibrium compositions of the two phases are known. Furthermore, assuming C atoms keep the same concentration in two phases (at  $r = p$ ) and B concentration profile jumps directly from zero to unity across the sharp  $\alpha/\beta$  interface at  $T = 0$  K, the above equation is reduced to,

$$\sigma = n_s \Delta e_{12} (1 - x_v^C)^2 \sum_j j Z_j \quad (11b)$$

Equation 11b indicates clearly that the addition of C atoms reduces the interfacial energy effectively in comparison with binary systems.

For a general case of  $r \neq p$  at  $T = 0$  K, C atoms have dissimilar interaction with A and B atoms, and thus have a tendency to stay solely in either  $\alpha$  or  $\beta$  phase according to the ratio of  $r/p$ . The interphase boundary can be regarded as  $A/B_{1-x}C_x$  or  $A_{1-x}C_x/B$  interfaces in some way (no ordered solution or intermetallics compound is considered to form here) according to the different affinity of C with A and B, and the interfacial energy is calculated as,

$$\begin{aligned} \sigma = n_s \Delta e_{12} (1 - x_\beta^C) \sum_j j Z_j - n_s \Delta e_{23} x_\beta^C (1 - x_\beta^C) \\ \times \sum_j j Z_j + n_s \Delta e_{13} x_\beta^C \sum_j j Z_j \end{aligned} \quad (11c)$$

and,

$$\begin{aligned} \sigma = n_s \Delta e_{12} (1 - x_\alpha^C) \sum_j j Z_j - n_s \Delta e_{13} x_\alpha^C (1 - x_\alpha^C) \\ \times \sum_j j Z_j + n_s \Delta e_{23} x_\alpha^C \sum_j j Z_j \end{aligned} \quad (11d)$$

for  $x_{\alpha}^C = 0$  and  $x_{\beta}^C = 0$ , respectively. It is noticed that all the above equations can be further reduced to match a binary system exactly [9].

### 3. Results and discussion

#### 3.1. Phase boundary composition

To begin with, solute atom C is first assumed to have similar bond energy with both A and B atoms, i.e. at  $r = p$ . The phase boundary composition corresponds to a symmetrical miscibility gap for such a case, as shown in the concentration triangle in Fig 1a. Various temperatures of 0.25, 0.5 and 0.75  $T_c$  are included in Fig 1a with  $r = p = -0.5$ , which implies that the regular interaction coefficient of A-C and B-C is negative and one half that of A-B. Below 0.25  $T_c$ , the  $\alpha$  phase contains almost only A and C atoms whereas the  $\beta$  phase is composed of B and C atoms solely if  $x^C$  is lower than about 0.4. With increasing C concentration and temperature as well, the dual phase region shrinks as in a binary system and the mixture of A and B atoms is pronounced. The maximum addition of C fraction to the alloy, which shows a miscibility gap, decreases from about 0.73 to 0.23 when temperature rises from 0.25  $T_c$  to 0.75  $T_c$ . It is interesting to point out that the maximum solubility of C in dual phase region is irrelevant with the value of  $r$  if  $r/p$  is fixed to unity. It is solely temperature dependent.

For the case of  $r \neq p$ , the shape of miscibility gap diverges from the symmetric case and the tie-lines tilt according to the ratio of  $r/p$ . Fig. 1b shows the phase boundary composition with tilted tie-lines at 0.5  $T_c$  for  $r = -0.5$  and  $p = -1$  for example. More C atoms are dissolved in  $\beta$  phase than in  $\alpha$  phase due to more negative  $p$  value. The miscibility gap is also enlarged slightly compared with  $r = p = -0.5$  at same temperature (dotted line in Fig 1b), which indicates that C atom rendering different A-C and B-C bonding energy promotes the separation of  $\alpha$  and  $\beta$  phase.

#### 3.2. Symmetric composition profile in the interphase boundary at $r = p$

The composition profiles can be calculated from each tie-lines calculated above for a given ternary alloy.

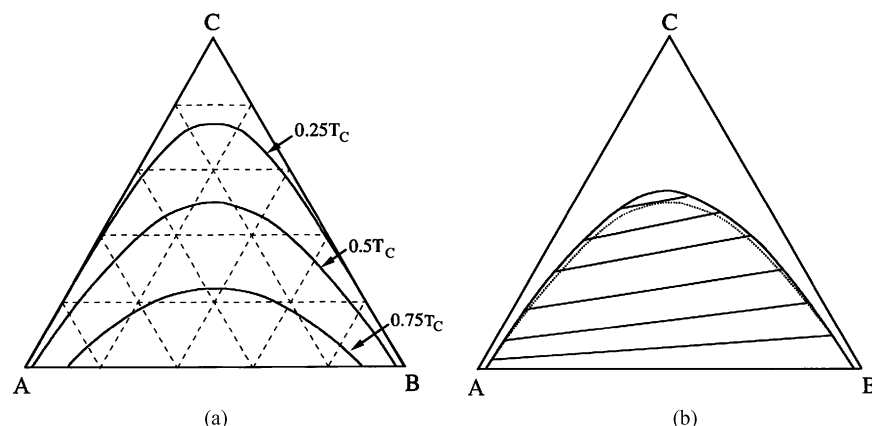


Figure 1 Calculated equilibrium  $\alpha/\beta$  phase boundary composition in A-B-C system of (a)  $r = p = -0.5$  at  $T = 0.25, 0.5$  and  $0.75 T_c$ , (b)  $r = -0.5$  and  $p = -1$  at  $T = 0.5 T_c$ , where  $r = \Delta e_{13}/\Delta e_{12}$  and  $p = \Delta e_{23}/\Delta e_{12}$ . The dashed line in (b) is that for  $r = p = -0.5$  at same temperature for comparison.

Fig. 2 show the profiles of A, B and C atoms at 0.25, 0.5 and 0.75  $T_c$ , respectively, which are calculated for a (100) interphase boundary in an alloy of nominal composition of  $x^C = 0.1$  with  $r = p = -0.5$ . The symmetric profiles for A and B are expectable from identical  $r$  and  $p$ , whereas the segregation of C atom in the interface region is worthy of noting. At a temperature of 0.25  $T_c$ , the concentration peak of C atom at the interface is more than twice that of bulk, as shown in Fig. 2a. The apparent variation of C concentration is limited to about four atomic layers. On the other hand, the mixture of A and B atoms is not significant at this temperature, except only for two adjacent layers. As temperature increases, the peak of C atom concentration decreases remarkably. At 0.75  $T_c$ , the C concentration shows negligible variation (less than 5%) across the interface zone, whereas the profiles of A and B atoms become relatively flat, which expands the interfacial zone to more than eight atomic layers.

Compared with the A-B binary system [9], it is seen that the concentration profiles of A and B atoms are generally more flat at the same temperature (eg. at 0.75  $T_c$  in Fig 2c), which indicates that the addition of C atoms into the system enhances the mixture of A and B atoms. At 0.25  $T_c$  (Fig 2a), the serious segregation of C atom in the interface brings even a small climax for A and B atoms in the nearest but one atomic layer to the exact interface. This may due to the effect of strong affinity of C to both A and B atoms despite of the repulsive interaction of A and B. As shown in Fig. 3a, for more attractive C atoms ( $r = -2$ ), the fluctuation on the profiles is more pronounced. If  $r$  is negative enough, the atom layers full of A or B atoms and accordingly depletion of C atoms are likely to present at interface. The significant oscillation profiles extending into both phases may suggest a tendency for ordering due to the negative  $r$  [16].

The influence of  $r$  on the composition profile is shown in Fig. 3 for a (100) interface at 0.25  $T_c$  with  $r = -2, 0, 0.3$ , respectively. In all the figures, apparent segregation of C atom into interface is indicated. It is seen that as the absolute value of  $r$  increases, the profile shape for A and B atoms gets flat. On the other hand, the concentration of C atoms at interface rises obviously, especially when  $r$  is positive. This means

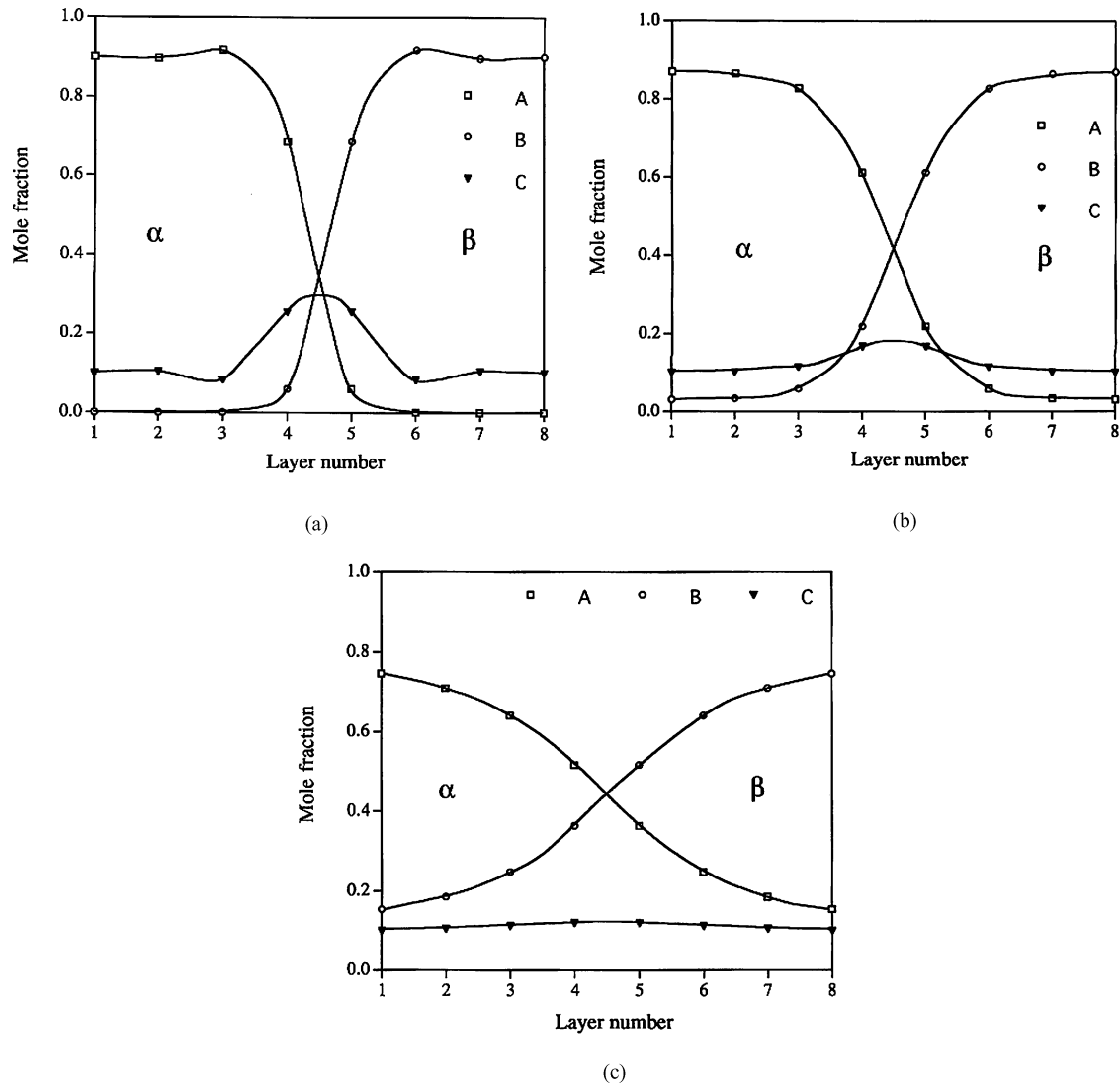


Figure 2 Composition profiles normal to (100) interface at (a)  $T = 0.25 T_c$ , (b)  $T = 0.5 T_c$  and (c)  $0.75 T_c$  with  $r = p = -0.5$  and  $x_\alpha^C = x_\beta^C = 0.1$ .

that C atoms which are repulsive with A and B atoms is more easier to segregate in the interface than that of attractive interaction, and renders a broader interface region. From this calculation, it is deduced that an interface composed of most C atoms develops reasonably when  $r$  is large enough. For example, if A-C, B-C and A-B have equal interactions ( $r = 1$ ), the  $\alpha/\beta$  interphase boundary is likely to be separated by a thin film of new  $\gamma$  phase containing main C atoms (actually  $\alpha/\gamma/\beta$  configuration occurs).

The relationship of maximum C concentration in the interphase boundary with respect to the ratio  $r (= p)$  is shown in Fig. 4 for various temperatures with a constant bulk C concentration of 0.1. The curves increase slowly with increasing  $r$  value, when  $r$  is more negative than  $-2$ , and rise abruptly after  $r$  is larger than approximate  $-1, 0$  and  $1$  for  $0.25 T_c, 0.5 T_c$  and  $0.75 T_c$ , respectively. It is also clear that the higher temperature, the lower C concentration peak, which is due to the dominant effect of entropy at elevated temperature.

Fig. 5 shows the unite concentration profile for (100), (110) and (111) boundary orientations with respect to the absolute distance from the interface at  $0.5 T_c$  and  $x^C = 0.1$ . The composition profile seems to be indepen-

dent of interface orientation, as in a binary alloy [9], which makes it possible to evaluate the concentration profile for any orientations from (100) readily.

### 3.3. Asymmetrical composition profile in the interphase boundary at $r \neq p$

In actual alloys,  $r$  is not usually equal to  $p$ , i.e.  $\Delta e_{13}$  is different from  $\Delta e_{23}$ . An asymmetrical concentration profile is shown in Fig. 6 at  $0.25 T_c$  for  $r = -0.5$  but  $p = -0.7, -0.25$  and  $0.5$ , respectively. At  $p = -0.7$ , B-C affinity is more stronger than that of A-C, the segregation of C atom in  $\beta$  phase is profound than that in  $\alpha$  phase. The peak of C occurs at the original  $\beta$  layer, in contrast to the symmetrical profile at  $r = p$  (Figs. 2 and 3). The oscillations in both C and B profiles are significant in  $\beta$  phase, which may imply the tendency of formation of BC intermetallic compound, whereas in  $\alpha$  phase the profiles are fairly regular. It is noticed that the bulk composition of C in  $\beta$  is higher than that in  $\alpha$  due to  $p/r > 1$  at this case. Alternatively at  $p = -0.25$  (Fig. 6b), which is less negative than  $r$ , an opposite propensity takes place compared with Fig. 6a. More C atoms present in  $\alpha$  phase rather than in  $\beta$  phase,

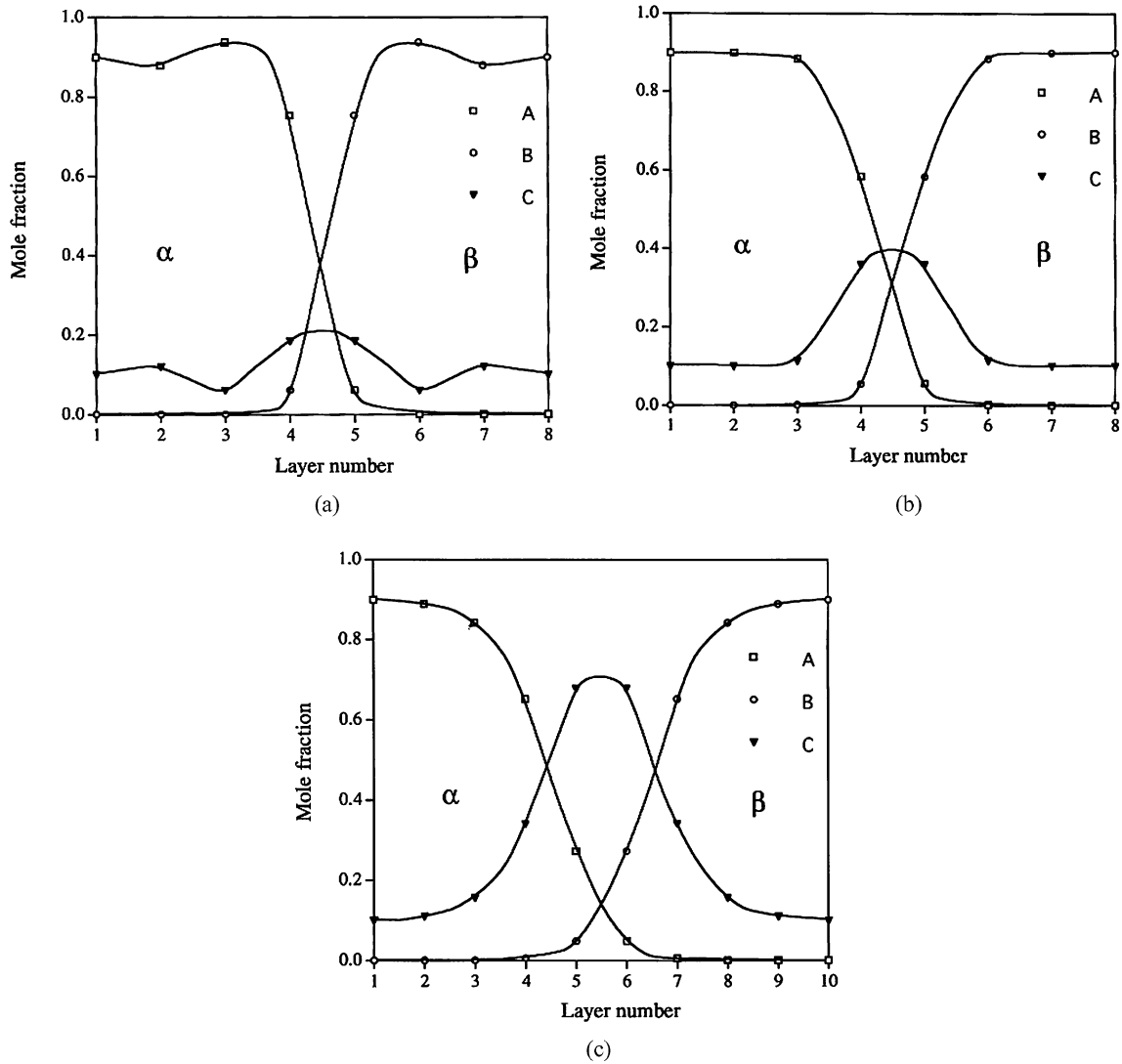


Figure 3 Composition profiles normal to (100) interface with (a)  $r = p = -2$ , (b)  $r = p = 0$  and (c)  $r = p = 0.3$  at  $T = 0.25 T_c$ , and  $x_\alpha^C = x_\beta^C = 0.1$ .

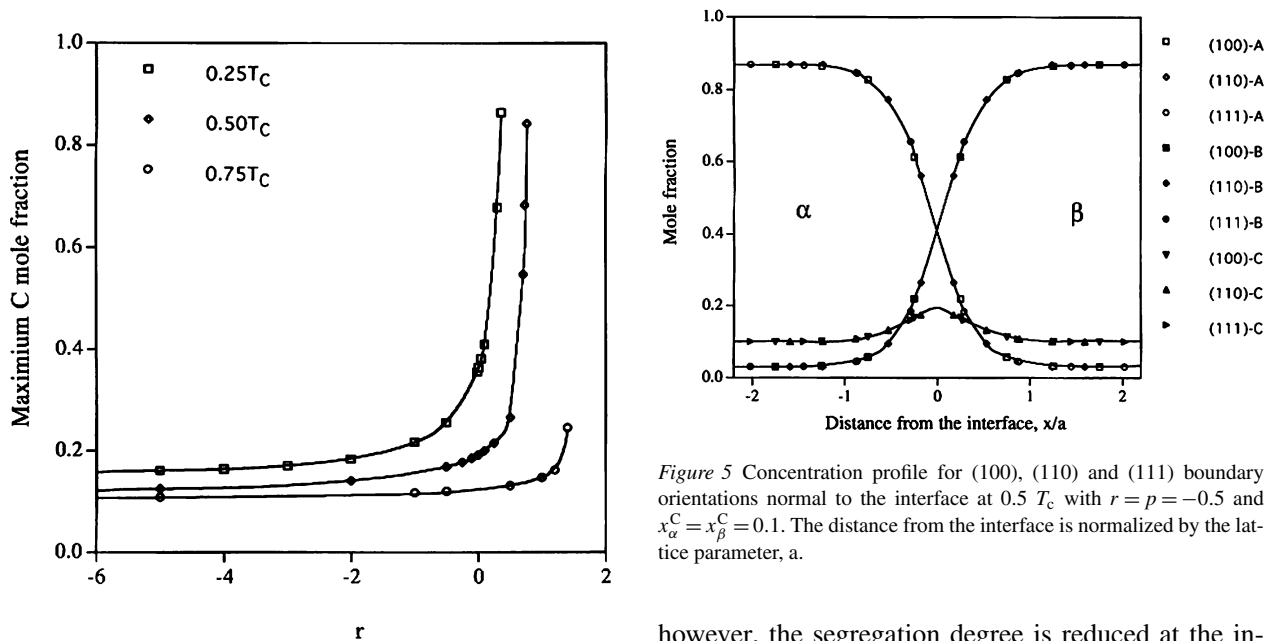


Figure 4 Variation of maximum C concentration in the interphase boundary with the ratio  $r$  at  $T = 0.25, 0.5$  and  $0.75 T_c$  and for a constant bulk C concentration of 0.1.

however, the segregation degree is reduced at the interfacial region, which is related to the actual value of  $r$  and  $p$ . If  $p$  is further increased to a positive number such as 0.5, most C atoms remain in  $\alpha$  phase with an

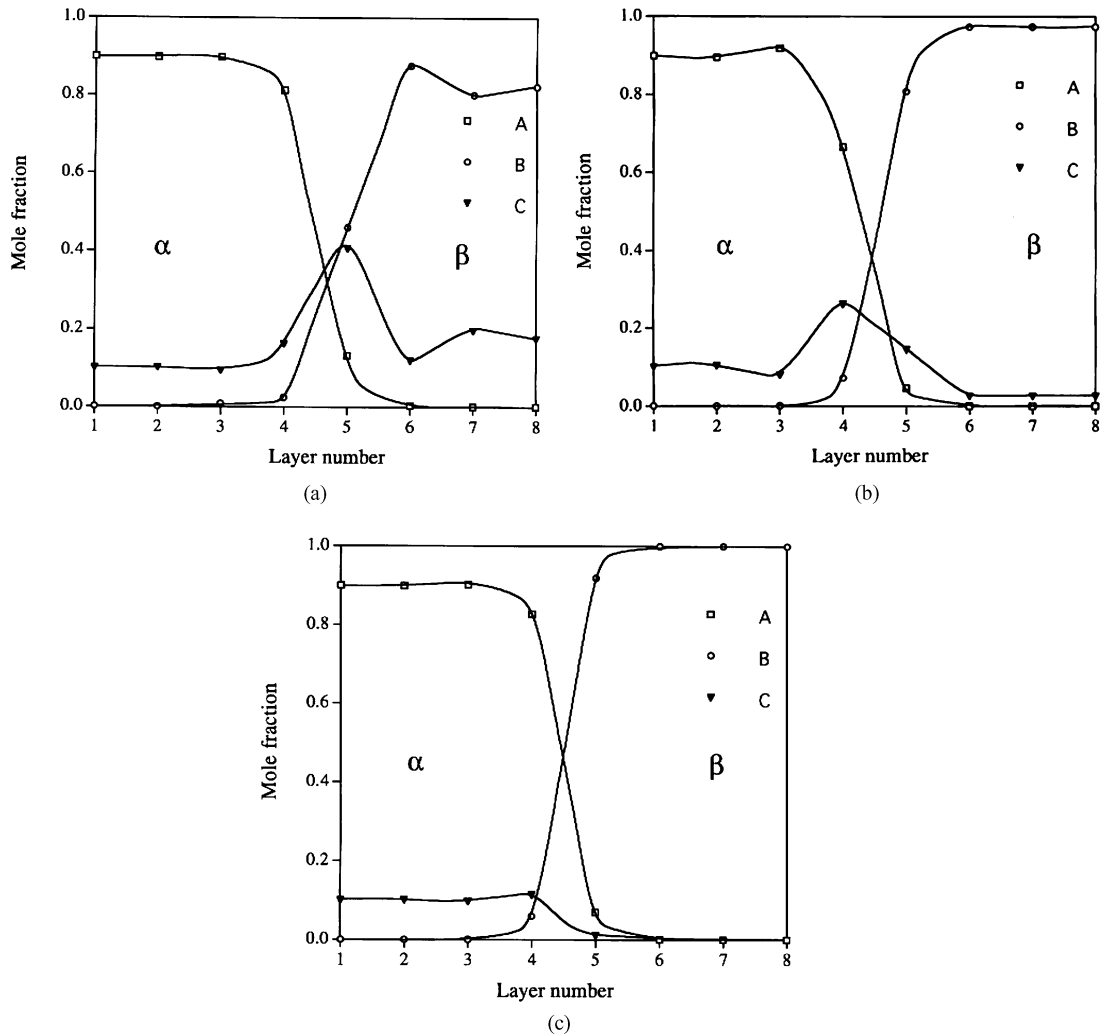


Figure 6 Concentration profile normal to (100) interface at  $0.25 T_c$  for  $r = -0.5$  but  $p = -0.7, -0.25$  and  $0.5$ , respectively.  $x_\alpha^C = x_\beta^C = 0.1$ .

abrupt drop to a negligible level cross the interface, as shown in Fig. 6c. The relatively sharp profiles of A, B and C atoms in Fig. 6c are owing to repulsive B-C and attractive A-C interaction concurrently.

### 3.4. Interfacial energy in ternary alloy

The (100) and (111) interfacial energy between  $\alpha$  and  $\beta$  phases for an alloy containing 0.1 C with  $r = p = -0.5$  (corresponding to the composition profiles in Fig. 2) was calculated and the results are shown in Fig. 7 in the unit of  $k_B T/a^2$ , where  $a$  is the lattice parameter. It is seen that the interfacial energy decreases rapidly with the increasing temperature, similar to a binary alloy ( $x^C = 0$ ). Since C atoms reduce the miscibility gap, the curves are terminated at temperature at which the alloy enters single phase field, which is much lower than  $T_c$  for A-B binary alloy.

The presence of third component atoms is shown clearly in Fig. 7 to decrease the interfacial energy compared with the binary system at same temperature. As mentioned above this is because C atoms decrease the composition gradient remarkably. The significant effect of C concentration on diminishing the interfacial energy is seen in Fig. 8 quantitatively for three temperatures with  $r = p = -0.5$ . This is reasonable from Equation 11b, which demonstrates a parabolic relationship of the energy with  $x^C$  at 0 K.

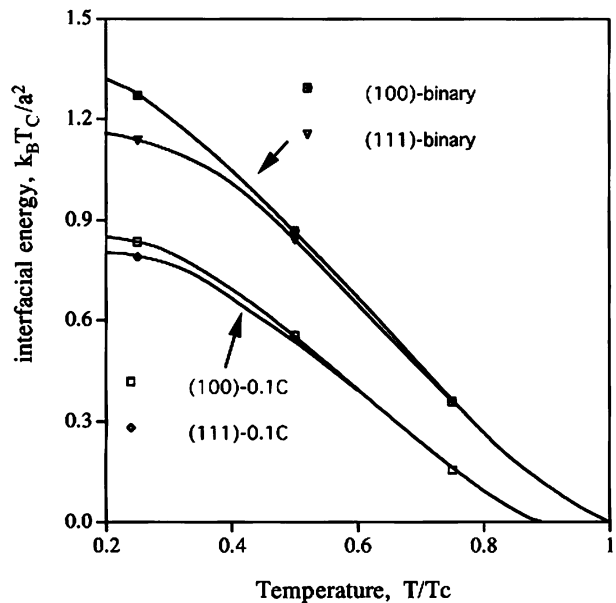


Figure 7 Variation of (100) and (111) interfacial energies in the unit of  $k_B T/a^2$  with temperature for the same ternary alloy as Fig. 2. The curves for binary system are also included for comparison.

For a constant value of  $x^C = 0.1$ , Fig. 9 shows the variation of (100) interfacial energy with the value of  $r (= p)$ . When  $r$  is negative, the interfacial energy shows a slight decrease with increasing  $r$ . When  $r$  is

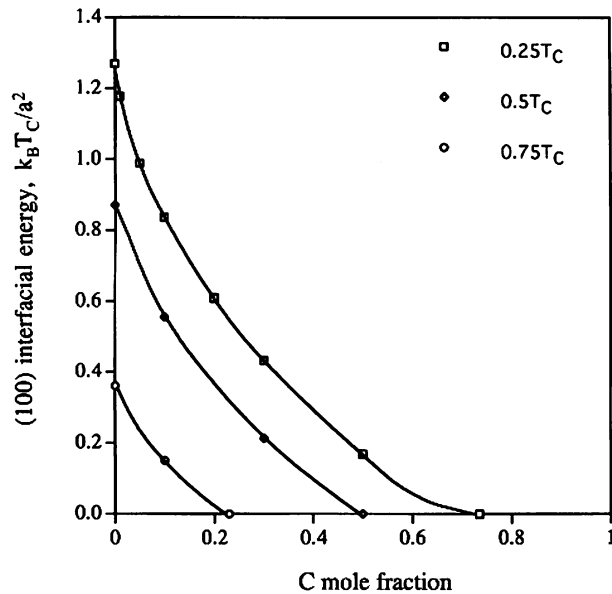


Figure 8 Effect of bulk C concentration on the interfacial energy for three temperatures with  $r = p = -0.5$ .

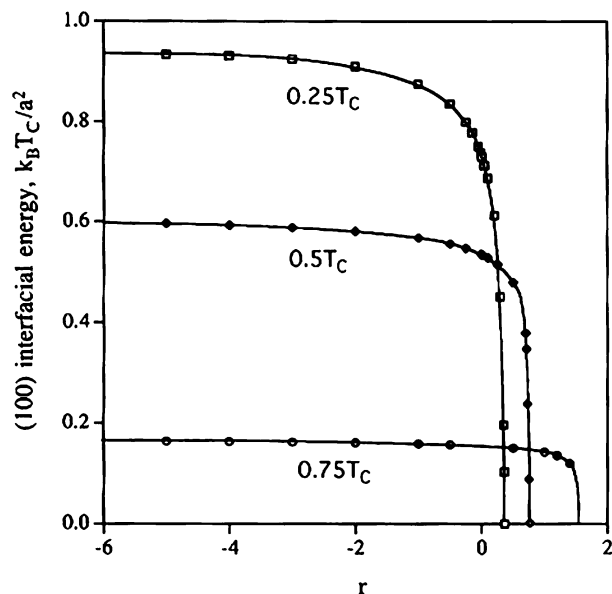


Figure 9 Variation of (100) interfacial energy with the value of  $r (= p)$  for a constant bulk C concentration of 0.1.

positive enough, an abrupt drop of the energy with increasing  $r$  occurs, which is consistent with the maximum C composition at the interface as shown in Fig. 4. This suggests that repulsive B-C and A-C interactions reduce the interfacial energy effectively.

At the case of  $r \neq p$ , the relationship of interfacial energy with  $p$  value is shown in Fig. 10 at  $0.25 T_C$  for  $r = -0.5$  and  $x_C^C = 0.1$ . With increasing  $p$  to a positive value, the B-C affinity decreases, and interfacial energy increases. This is because that the solubility of C atoms in  $\beta$  is reduced at such a case and the composition profiles are relatively sharp as shown in Fig. 6c for example. Thus C atom, which is attractive to one phase and repulsive to the other phase, is likely to result in an improved interfacial energy than identical B-C and A-C interaction.

The anisotropy of the interfacial energy in this ternary system is considered from Equations 11 to be same as

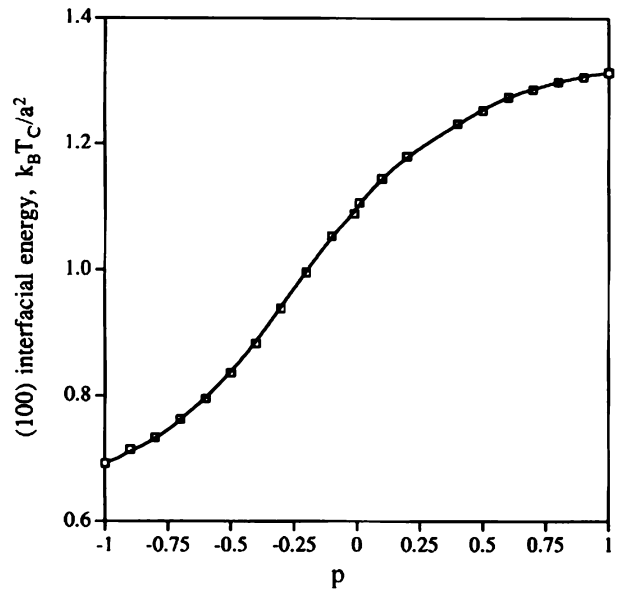


Figure 10 Relationship of (100) interfacial energy with  $p$  at  $0.25 T_C$  with  $r = -0.5$  and  $x_C^C = 0.1$ .

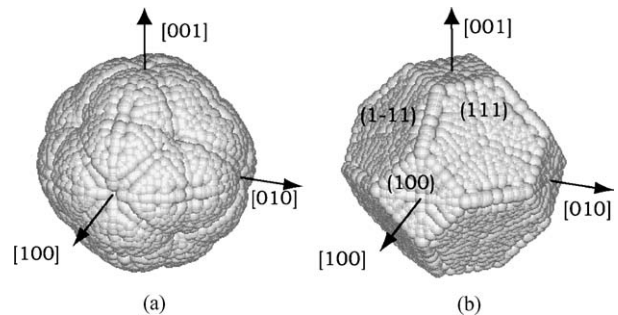


Figure 11 The 3-dimensional polar plot of interfacial energy and equilibrium shape from Wulff construction at  $T = 0$  K for an fcc ternary system.

that in a binary system at  $T = 0$  K, i.e.  $\{111\}$  has the smallest and  $\{210\}$  has the largest energy [9]. This is in sharp contrast for a ternary system containing interstitial atoms [11], whereas  $\{111\}$  has the largest energy and the precipitate basically has an equilibrium cube shape [12]. The 3-dimensional polar plot and Wulff construction of interfacial energy for the present A-B-C ternary system is shown in Fig. 11 at  $T = 0$  K [18]. The equilibrium shape is a tetradecahedron with dominated  $\{111\}$  facets and minor  $\{100\}$  facets. As temperature increases, the anisotropy of energy decreases and eventually isotropic sphere-shaped equilibrium precipitates is preferential at temperatures high enough. The favorable  $\{111\}$  facets is consistent with a Monte-Carlo study of the same alloy [19], which indicates also the presence of  $\{111\}$  facets for the protrusion at the interface.

### 3.5. Application to Cu-Ag-Au alloy

A Cu-Ag-Au alloy may be one obvious example for application of the above calculation. Copper, silver and gold are in fcc structure, with the lattice parameter of 0.362, 0.409 and 0.408, respectively [20]. Cu-Ag interaction is positive, and the critical temperature of miscibility gap,  $T_C$ , is calculated to be 1913 K from the mixing enthalpy [20]. The negative regular solution



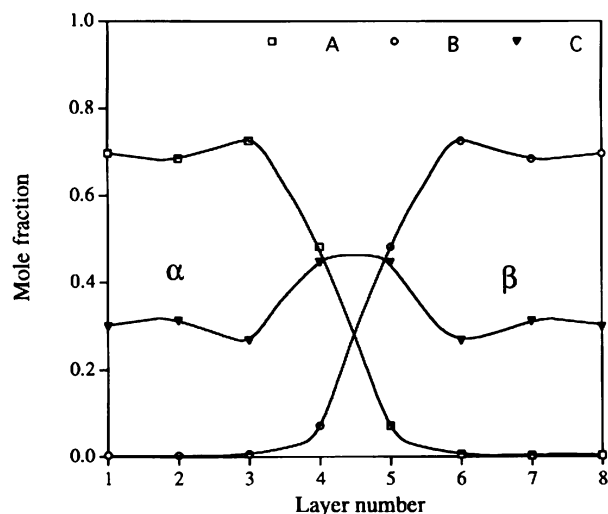


Figure 12 Concentration profile normal to (100) interface at  $0.25 T_c$  for  $r = p = -0.5$  and  $x_a^C = x_b^C = 0.3$ .

constant of Cu-Au and Ag-Au is nearly equal (about 10% difference) [21], and about 1/2 of that of Cu-Ag ( $r = p = -0.5$ ). For such a system at 580 K, the measured distribution of gold by scanning Auger spectroscopy [1] shows clearly the segregation of Au at Cu/Ag interface region to such a degree, which agrees with present calculation in general (Fig. 12). Unfortunately, the comparison is rather qualitatively than quantitatively, since the calculation indicates the profile across only several atomic layers (totally distance less than 20 nm), which may be quite difficult to demonstrate by experiments. The experimental asymmetric profiles at a much broad interface [1] are owing to the strain energy arising from the lattice misfit [16]. The segregation of Au atoms tends to be suppressed on the Cu-rich phase because of greater size misfit and enhanced on the Ag-rich phase accordingly.

#### 4. Summary

The discrete lattice plane/nearest neighbor broken bond model was employed to calculate the composition profile and the interfacial energy in a ternary substitutional fcc system. The equations of solute distribution, which were developed following the scheme reported previously in a binary system [9], were solved to calculate the temperature and composition assuming various interaction parameters.

The third component atoms, C, which have same interaction with A and B atoms, render symmetric composition profiles across the interface. C atoms have a strong propensity to segregate at the  $\alpha/\beta$  interface, and reduce the interfacial energy compared with corresponding binary alloy. The segregation of C atoms and reduction of energy are more significant for repulsive A-C and B-C interaction than negative A-C and B-C interaction. The calculated data are in fairly agreement with the experimental result in a Cu-Ag-Au alloy.

As temperature increases, the gradient of composition profiles for A, B and C and interfacial energy decrease in a similar way with a binary alloy. A Becker-

type expression was derived which allows one to estimate the chemical interfacial energy in A-B-C ternary system at lower temperatures once bulk equilibrium phase boundaries and bond energies are known. The anisotropy of the interfacial energy in ternary systems at  $T = 0$  K is same as in the corresponding binary system, and decreases rapidly with increasing temperature as well as the bulk concentration of C atoms.

In case of different A-C and B-C interaction, asymmetric concentration profiles present at the interface. The segregation of C atoms is more intensive in the phase which contains more attractive atoms to C relative to the other. As the difference of A-C and B-C interaction enlarges to a sufficient amount, a configuration of AC/B or A/BC interphase boundary is expected to occur.

#### Acknowledgements

The authors are grateful to the support from Specialized Research Fund for the Doctoral Program of Higher Education in P. R. China, National Natural Science Foundation of China under No. 50201007, and Materials Science and Engineering Research Center of Jiangxi Province in P. R. China as well.

#### References

1. S. A. DREGIA, P. WYNBLATT and C. L. BAUER, *J. Vac. Sci. Technol. A* **5** (1987) 1746
2. G. GAO, D. B. ZHANG and P. WYNBLATT, *Acta Metall. Mater.* **41** (1993) 3331.
3. A. P. SUTTON and R. W. BALLUFFI, "Interfaces in Crystalline Materials, Monographs on the Physics and Chemistry of Materials," Clarendon Press, Oxford, 1995, vol. 51.
4. J. M. HOWE, "Interfaces in Materials" (John Wiley & Sons, Inc., 1997).
5. R. BECKER, *Annln. Phys.* **32** (1938) 128.
6. S. ONO, *Mem. Fac. Engng., Kyushu Univ.* **10** (1947) 195.
7. M. HILLERT, *Acta Metall.* **9** (1961) 525.
8. J. L. MEIJERING, *ibid* **14** (1966), 251.
9. Y. W. LEE and H. I. AARONSON, *ibid* **28** (1980) 539.
10. J. W. CAHN and J. E. HILLIARD, *J. Chem. Phys.* **28** (1958) 258.
11. Z.-G. YANG and M. ENOMOTO, *Acta Mater.* **47** (1999) 4515.
12. *Idem.*, *Metall. Mater. Trans.* **32A** (2001) 267.
13. *Idem.*, *Mater. Sci. Eng. A.* **332** (2002) 184.
14. W. C. JOHNSON and J. M. BLAKELY (eds.), "Interfacial Segregation" (Am. Soc. Metals, Metals Park, Ohio, 1979).
15. J. W. GIBBS, "The Scientific Papers of J. Willard Gibbs," (Dover, New York, 1961) vol. 1.
16. S. A. DREGIA and P. WYNBLATT, *Acta Metall. Mater.* **29** (1991) 771.
17. S. M. FOILES, M. I. BASKES and M. S. DAW, *Phys. Rev. B*, **33** (1986) 7983.
18. Z.-G. YANG and M. ENOMOTO, unpublished work.
19. P. BACHER, P. WYNBLATT and S. M. FOILES, *Acta Metall. Mater.* **39** (1991) 2681.
20. B. D. CULLITY, "Elements of X-ray Diffraction" 2nd ed. (Addison-Wesley, Reading, MA, 1978).
21. R. HULTGREN, P. D. DESAI, D. T. HAWKINS, M. GLEISER and K. K. KELLY, "Selected Values of Thermodynamic Properties of Binary Alloys" (ASM, Metals Park, OH, 1973).

Received 14 January

and accepted 20 September 2004